Kinetic-equation approach to diffusive superconducting hybrid devices

T. H. Stoof and Yu. V. Nazarov
Faculty of Applied Physics and Delft Institute for Microelectronics and Submicron Technology, Delft University of Technology, Lorentzweg 1, 2628 CJ Delft, The Netherlands
(Received 18 January 1996)

We present calculations of the temperature-dependent electrostatic and chemical potential distributions in disordered normal metal-superconductor structures. We show that they differ appreciably in the presence of a superconducting terminal and propose an experiment to measure these two different potential distributions. We also compute the resistance change in these structures due to a recently proposed mechanism which causes a finite effect at zero temperature. The relative resistance change due to this effect is of the order of the interaction parameter in the normal metal. Finally a detailed calculation of the resistance change due to the temperature dependence of Andreev reflection in diffusive systems is presented. We find that the maximal magnitude due to this thermal effect is in general much larger than the magnitude of the interaction effect. [S0163-1829(96)08521-9]

I. INTRODUCTION

Mesoscopic structures in which normal metal wires or semiconductors are attached to superconductors have received a fair amount of attention in the past few years. In particular devices known as Andreev interferometers, in which two superconducting terminals with different macroscopic phases are present, have been in the focus of interest. The conductance of these structures, in which electrons and holes undergo multiple Andreev reflection depends on the phase difference of the connected superconductors, hence the name Andreev interferometry.

Since the prediction of Andreev reflection,[1] the theory of charge transport through N-S junctions has been well established.[2–4] However, the practical implications of this phenomenon for the sophisticated nanostructures that can nowadays be realized are not always clear. The reason for this is the coherent nature of multiple Andreev reflection which determines the physical behavior of these devices. These technological developments resulted in the current revival of the topic in mesoscopic physics.

In the last few years a large number of Andreev interferometers have been studied both theoretically[5–11] and experimentally.[12–15] Particularly the experiment of Ref. 15 motivated the research presented here. In this experiment, the resistance of a cross shaped diffusive normal metal was measured. The two branches of the cross perpendicular to the current path were in contact with a large superconducting loop. The phase difference between the superconducting end points of the loop could be controlled by a small current through the loop or, alternatively, by applying a magnetic field. The resistance of the structure oscillated nonharmonically as a function of the phase difference by about 10% of the normal state resistance. These results were unexpected because in the conventional theory of the proximity effect, in which electron-electron interactions in the normal metal region are disregarded, the zero-voltage, zero-temperature resistance of a diffusive metal is predicted to be phase independent.[16,17] Furthermore, the large amplitude and the observed 2π periodicity ruled out the possibility of a weak localization effect, since the latter was predicted to show a phase dependence with a fundamental period of π.[18,19] To this day, resistance oscillations with π periodicity remain unobserved.

Recently we proposed a mechanism which provides a phase-dependent resistivity in a diffusive conductor at zero temperature.[17] This scheme takes into account the fact that the electron-electron interaction induces a weak pair potential in the normal metal. As a result, Andreev reflection occurs in the entire structure, rather than only at the N-S interfaces. This results in a phase-dependent resistance change which is proportional to the interaction parameter λ in the normal metal and can be of either sign, depending on the sign of λ. Although the experiment of Ref. 15 could be explained in terms of the proximity effect theory and the results were shown to be caused by the finite temperature at which the experiments were performed,[17] it would be challenging to observe the resistance oscillations predicted in Ref. 17. This would also be of practical interest since it would provide the means to directly measure the interaction parameter in the normal metal. However, in addition to the fact that electron-hole coherence influences the resistance, it also manifests itself in a nontrivial distribution of the electrostatic and chemical potentials in the structure as we will show below.

The remainder of this paper is organized as follows. In Sec. II we briefly discuss the influence of phase coherence on transport properties and potential distributions in small diffusive structures. Section III contains the theoretical foundation of our calculations. We first review the relevant techniques of the Keldysh formalism for diffusive superconductors and then derive the equations for the Green functions and distribution functions which determine the electric transport properties of the system. The next three sections are devoted to several applications of the theory. We first calculate the temperature-dependent electrostatic and chemical potential distributions in a simple one-dimensional structure in Sec. IV. A second application is presented in Sec. V, where we calculate the resistance change at zero temperature due to the induced pair potential in the normal

metal region for two experimentally relevant geometries. The third and last application is discussed in Sec. VI. There we focus our attention on the influence of a finite temperature on the resistance in these structures. Some of the results in Secs. V and VI were published in a preliminary form in Ref. 17. However, here we additionally give a detailed description of the performed calculations. We summarize our conclusions in Sec. VII.

II. COHERENCE EFFECTS IN ULTRASMALL DISORDERED STRUCTURES

Owing to the advance in nanofabrication techniques over the past years, the fabrication of hybrid metallic superconducting structures with a characteristic size of a few microns or less has nowadays become possible. If these small structures are at a sufficiently low temperature, the quasiparticles in the metal can no longer penetrate into the superconductor due to the large superconducting gap. As a result, the lowest-order process that determines the resistance of the system is Andreev reflection, in which an electron is reflected as a hole or, alternatively, in which an electron pair enters the superconductor. This reflection causes electrons and holes in the diffusive metal to be phase coherent over distances of the order of $\xi=\sqrt{\mathscr{D}/T}\gg l$, where $\mathscr{D}=\frac{1}{3}v_F l$ is the diffusion constant and l is the elastic mean free path.

This phase coherence between electrons and holes drastically alters the physics of transport through such systems. The most striking feature is that the electrostatic potential and nonequilibrium chemical potential are no longer distributed linearly through the sample. The nonlinearity of the electrostatic potential implies a nonuniform resistivity distribution and consequently a nonlocal resistance of the structure. This nonlocality is a fundamental feature of the coherent nature of Andreev reflection. Moreover, at finite temperatures the transport properties of the system cease to be distributed uniformly over all energies. Hence, a calculation of these quantities, to which the main part of this article will be devoted, must first consider them at each energy individually and then integrate over all energies.

Another manifestation of the phase coherence in the normal metal is the difference in the distribution functions of the electrostatic and chemical potentials. In a normal system both would be equal, but this changes when one of the leads is brought into the superconducting state. Whereas the former is simply determined by the distribution of charge in the system, the latter can only be defined for small perturbations from equilibrium, i.e., when the quasiparticle energies are much smaller than the superconducting gap. To show how this definition comes about we consider the normal current through a disordered *N-I-S* junction. Zhou, Spivak, and Zyuzin showed that for small quasiparticle energies ε this current can be written in the following way:[20]

$$j(\varepsilon,x_N)=t\{f_T(\varepsilon,x_S)-f_T(\varepsilon,x_N)\}F(\varepsilon,x_N,x_S), \quad (2.1)$$

where t is the transparency of the tunnel barrier, x_N and x_S denote the normal-metal side and superconducting side of the barrier, F is some function of ε, x_N and x_S, and f_T is the nonequilibrium distribution function. This equation shows that at low temperatures the nonequilibrium chemical potential can be associated with the distribution function and consequently that it is a measurable quantity. As will be discussed in Sec. IV, the electrostatic potential decreases faster than linear in the vicinity of the superconductor due to the decreased density of states near the *N-S* interface. In contrast, the chemical potential changes only a little in the presence of a superconducting terminal and consequently the ratio of the electrostatic and chemical potential vanishes near the superconductor.

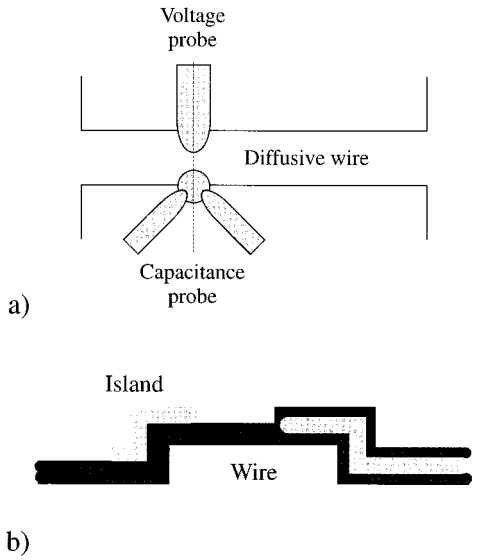

FIG. 1. Schematic setup of an experiment to measure the electrostatic and chemical potential: (a) Top view. (b) Cross section along the dashed line in (a). For details, see text.

A possible experimental setup to measure the difference between the electrostatic and chemical potential is drawn in Fig. 1. The figure shows a diffusive wire connecting two reservoirs (not shown) in the presence of two different probes. The voltage probe measures the chemical and the capacitance probe the electrostatic potential. As shown in Fig. 1(b), the voltage probe consists simply of a metallic lead separated from the wire by a thin oxide layer. The latter is indicated by the dark shaded region. The capacitance probe is slightly more complicated. In principle one could use a single metallic gate separated by a thick oxide layer to reduce tunneling from lead to wire. However, because such a gate would not only couple capacitively to the charge in the wire directly underneath the tip but also strongly to the surroundings, we propose a slightly different method: A small metallic island is deposited on the edge of the wire as indicated in the figure. This island is weakly coupled to two extra leads through which a current can flow. In this case the electrostatic potential capacitively induces a charge on the island, thus very sensitively changing the measured Coulomb threshold. Both probes can be calibrated since they should measure the same potentials if both reservoirs are in the normal state. If one of the reservoirs is brought into the superconducting state, both potentials should change. If one would attach different probes along the wire it would be possible to measure the potential landscapes in the wire. In Sec. IV we will return to this subject in a more quantitative fashion, but we will now first discuss the necessary theory.

III. METHOD

A. Kinetic equations for the distribution functions in the dirty limit

To describe the system we use the nonequilibrium Green function method derived by Keldysh[21] and later further developed for superconductivity by Larkin and Ovchinnikov.[22] Although this framework is rather formal it has one large advantage over, e.g., the scattering approach. As was mentioned above the resistance of the structure is nonlocal. However, using the Keldysh technique it is possible to express scattering processes in the structure as well as other relevant physical quantities, like the resistance, in terms of local Green functions in coincident points. This property of the formalism simplifies the calculations considerably. To establish notation and to remind the reader of the basic theory we briefly review the essential ingredients of the Keldysh formalism and the quasiclassical approximation for diffusive superconductors. For more extensive reviews, we refer to, e.g., Refs. 23 and 24.

In this formalism the Green function is given by the (4×4) matrix

$$\check{G}=\begin{pmatrix}\hat{G}^R & \hat{G}^K\\ 0 & \hat{G}^A\end{pmatrix}, \tag{3.1}$$

where $\hat{G}^A,\hat{G}^R$, and $\hat{G}^K$ are the advanced, retarded, and Keldysh Green function which are (2×2) matrices in Nambu space given by[25]

$$\hat{G}^A(1,1')=\begin{pmatrix}G^A(1,1') & F^A(1,1')\\ F^{A\dagger}(1,1') & -G^A(1',1)\end{pmatrix}, \tag{3.2}$$

and analogous equations for $\hat{G}^R$ and $\hat{G}^K$. Throughout this article the symbol ''check'' will be used to denote (4×4) matrices and ''hat'' for (2×2) matrices. The normal and anomalous Green function are given by:

$$G^R(1,1')=-i\,\theta(t_1-t_{1'})\langle[\psi(1),\psi^\dagger(1')]_+\rangle, \tag{3.3a}$$

$$G^A(1,1')=i\,\theta(t_{1'}-t_1)\langle[\psi(1),\psi^\dagger(1')]_+\rangle, \tag{3.3b}$$

$$G^K(1,1')=-i\langle[\psi(1),\psi^\dagger(1')]\rangle, \tag{3.3c}$$

$$F^R(1,1')=-i\,\theta(t_1-t_{1'})\langle[\psi(1),\psi(1')]_+\rangle, \tag{3.3d}$$

$$F^A(1,1')=i\,\theta(t_{1'}-t_1)\langle[\psi(1),\psi(1')]_+\rangle, \tag{3.3e}$$

$$F^K(1,1')=i\langle[\psi^\dagger(1),\psi^\dagger(1')]\rangle, \tag{3.3f}$$

where $\psi(1)=\psi(t_1,\mathbf{r}_1)$ is the electron field operator.

We proceed by introducing the center-of-mass and relative coordinates $\mathbf{r}=\frac{1}{2}(\mathbf{r}_1+\mathbf{r}_{1'})$ and $\mathbf{r}'=\mathbf{r}_1-\mathbf{r}_{1'}$ and by Fourier transforming the Green function with respect to the relative coordinate: $\check{G}(\mathbf{r},\mathbf{p})=\int d\mathbf{r}'\exp(-i\mathbf{p}\mathbf{r}')\check{G}(\mathbf{r}+\frac{1}{2}\mathbf{r}',\mathbf{r}-\frac{1}{2}\mathbf{r}')$. We apply the quasiclassical approximation, which is based on the fact that the Fermi energy in the system is much larger than all other energy scales. This means that all relevant physical quantities vary spatially on a length scale that is much larger than the Fermi wavelength. In this case it is useful to introduce the so-called quasiclassical Green function $\check{g}$ which is integrated over $\xi_{\mathbf{p}}=\mathbf{p}^2/2m-\mu$:

$$\check{g}(\mathbf{r},\hat{p},t_1,t_{1'})=\frac{i}{\pi}\int d\xi_{\mathbf{p}}\check{G}(\mathbf{r},\mathbf{p},t_1,t_{1'}). \tag{3.4}$$

Here $\hat{p}$ in the left-hand side denotes the fact that the momentum dependence of the quasiclassical Green function is restricted to dependence on the direction of $\mathbf{p}$ only. In this approximation the magnitude of the momentum is fixed at $|\mathbf{p}|=p_{\mathrm{F}}$. This quasiclasissical Green function satisfies the normalization condition

$$\int dt_{1''}\check{g}(t_1,t_{1''})\check{g}(t_{1''},t_{1'})=\check{1}\delta(t_1-t_{1'}). \tag{3.5}$$

In the case of a superconductor with short elastic mean free path, i.e., in the diffusive regime, it is feasible to expand the Green function to first order in spherical harmonics:[26]

$$\check{g}=\check{g}_s+\mathbf{p}\check{\mathbf{g}}_p,\quad \mathbf{p}\check{\mathbf{g}}_p\ll\check{g}_s, \tag{3.6}$$

where the functions $\check{g}_s$ and $\check{\mathbf{g}}_p$ no longer depend on the direction of $\mathbf{p}$. Using the normalization condition (3.5) we find an expression for $\check{\mathbf{g}}_p$, which is then substituted back into Eq. (3.6). The thus obtained Green function is then averaged over all angles of $\mathbf{p}$. In the stationary case, the Green function depends on the time difference $\tau=t_1-t_{1'}$ only. Performing the Fourier transform with respect to this time difference, we obtain the equation of motion for the Green function $\check{g}_\varepsilon=\int d\tau\check{g}_s(\tau)\exp(i\varepsilon\tau)$ (we drop the index s from now on)[27]

$$-\mathscr{D}\boldsymbol{\nabla}(\check{g}_\varepsilon\boldsymbol{\nabla}\check{g}_\varepsilon)+i[\check{H},\check{g}_\varepsilon]+i[\check{\Sigma},\check{g}_\varepsilon]=0, \tag{3.7a}$$

$$\check{g}_\varepsilon^2=\check{1}, \tag{3.7b}$$

where $\mathscr{D}=\frac{1}{3}v_F l$ is the diffusivity, l is the elastic mean free path, $\check{H}=e\varphi\check{1}+\varepsilon\check{\sigma}_z-\check{\Delta}$ and $\check{\Delta}$ and $\check{\sigma}_z$ are given by

$$\check{\Delta}=\begin{pmatrix}\hat{\Delta} & 0\\ 0 & \hat{\Delta}\end{pmatrix},\quad \hat{\Delta}=\begin{pmatrix}0 & \Delta\\ -\Delta^* & 0\end{pmatrix}, \tag{3.8}$$

where Δ is the pair potential in the metal and

$$\check{\sigma}_z=\begin{pmatrix}\hat{\sigma}_z & 0\\ 0 & \hat{\sigma}_z\end{pmatrix},\quad \hat{\sigma}_z=\begin{pmatrix}1 & 0\\ 0 & -1\end{pmatrix}. \tag{3.9}$$

In Eq. (3.7a) elastic non-spin-flip impurity scattering has been taken into account in the Born approximation, causing the presence of the elastic mean free path l in the diffusion constant.[24] Hence, the self-energy matrix $\check{\Sigma}$ in Eq. (3.7a), which has the same structure as the Green function (3.1), takes into account processes such as spin-flip scattering and the inelastic scattering of electrons with phonons and (magnetic) impurities.

The general expression for the electrostatic potential φ in Eq. (3.7a), which follows from electroneutrality in the metal, is[24,20]

$$\varphi(x)=-\frac{1}{8e}\int_{-\infty}^{\infty}d\varepsilon\ \mathrm{Tr}\hat{g}_\varepsilon^{\mathrm{K}}(x). \tag{3.10}$$

Throughout this article the electrostatic potential is assumed to be time independent.

The advanced and retarded Green functions determine the dispersion of the quasiparticles. However, to solve a transport problem we need to know how the energy spectrum is filled by extra quasiparticles when the system is driven out of equilibrium. This is determined by the Keldysh component $\hat{g}^K$ of $\check{g}$, which can be expressed in the advanced and retarded ones using two distribution functions:[22–24]

$$\hat{g}^K_\varepsilon = \hat{g}^R_\varepsilon \hat{f} - \hat{f}\hat{g}^A_\varepsilon \tag{3.11a}$$

$$\hat{f} = f_L \hat{1} + f_T \hat{\sigma}_z . \tag{3.11b}$$

In a spatially slowly varying electromagnetic field, the equations for the two distribution functions are (dropping collision integrals because they account for inelastic scattering processes, and time derivatives because we seek to find stationary solutions only)

$$\mathscr{D}\boldsymbol{\nabla}\ \mathrm{Tr}\{\boldsymbol{\nabla} f_L(\hat{1} - \hat{g}^R_\varepsilon \hat{g}^A_\varepsilon)\} + \mathscr{D}\boldsymbol{\nabla}(f_T j_\varepsilon) = 0, \tag{3.12a}$$

$$\mathscr{D}\boldsymbol{\nabla}\ \mathrm{Tr}\{\boldsymbol{\nabla} f_T(\hat{1} - \hat{\sigma}_z \hat{g}^R_\varepsilon \hat{\sigma}_z \hat{g}^A_\varepsilon)\} + \mathscr{D}\boldsymbol{\nabla} f_L j_\varepsilon \tag{3.12b}$$

$$+ 2if_T \mathrm{Tr}\{(\hat{g}^R_\varepsilon + \hat{g}^A_\varepsilon)\hat{\Delta}\} = 0, \tag{3.12c}$$

where $j_\varepsilon = \mathrm{Tr}\hat{\sigma}_z\{\hat{g}^R_\varepsilon \hat{\partial}\hat{g}^R_\varepsilon - \hat{g}^A_\varepsilon \hat{\partial}\hat{g}^A_\varepsilon\}$.

To close the set of equations we finally need an equation for the pair potential in the normal metal region. This expression for Δ can be derived from the self-consistency relation:

$$\hat{\Delta}(\mathbf{r}) = \frac{\lambda}{4i}\int d\varepsilon \{\hat{g}^K_\varepsilon(\mathbf{r}, \hat{p}, \tau)\}_{o\text{-}d},$$

$$= \frac{\lambda}{4i}\int d\varepsilon\ \tanh\left(\frac{\varepsilon}{2T}\right)\{\hat{g}^R_\varepsilon - \hat{g}^A_\varepsilon\}_{o\text{-}d}, \tag{3.13}$$

where $\lambda = gN(0)$ is the interaction parameter, g, times the density of states at the Fermi level, $N(0)$. The subscript o-d denotes the off-diagonal part.

This concludes the derivation of the distribution functions. We now have a closed system of equations that in principle must be solved self-consistently. In the next section we will discuss specific circumstances that allow for a simplification of the equations, enabling us to solve them perturbatively.

B. Approximations

In this section we discuss the assumptions and approximations that enable us to simplify the theory. We subsequently derive the final set of equations that we will use.

We start by noting that Eq. (3.7a) for the Green function still contains the self-energy matrix $\check{\Sigma}$. However, because we are only interested in the case where the phase breaking length is much larger than the system size, it is reasonable to disregard inelastic scattering processes and hence, we neglect $\check{\Sigma}$ from now on. Eq. (3.7a) then reduces to[17]

$$\mathscr{D}\boldsymbol{\nabla}(\check{g}_\varepsilon \boldsymbol{\nabla}\check{g}_\varepsilon) - i[\check{H}, \check{g}_\varepsilon] = 0. \tag{3.14}$$

We now have equations for the diagonal components $\hat{g}^A_\varepsilon$ and $\hat{g}^R_\varepsilon$ of the Green function (3.1).

We parametrize the advanced Green function in the following way:

$$\hat{g}^A_\varepsilon = \begin{pmatrix} \cos\theta & ie^{i\phi}\sin\theta \\ -ie^{-i\phi}\sin\theta & -\cos\theta \end{pmatrix}, \tag{3.15}$$

thus ensuring that $\hat{g}^2_\varepsilon = \hat{1}$. In general ϕ and θ are complex and depend on energy and position. In a structure with two superconducting terminals, $\hat{g}^A_\varepsilon$ will depend on the phase *difference* $\phi_1 - \phi_2$ between the two superconductors. However, if only one superconducting reservoir is present, the resistance of the structure will not depend on the absolute phase and we can put $\phi = 0$.

In the case of sufficiently small quasiparticle, thermal and Thouless energies; $\varepsilon, k_B T, \mathscr{D}/L^2 \ll \Delta_S$, where Δ_S is the energy gap in the superconductor, the advanced Green function can be written in the following way:[22]

$$\hat{g}^A_\varepsilon = \frac{-1}{\sqrt{(\varepsilon - i\delta)^2 - |\Delta|^2}}\begin{pmatrix} \varepsilon & \Delta \\ -\Delta^* & -\varepsilon \end{pmatrix}, \tag{3.16}$$

where δ is an infinitesimally small positive number. Using this representation for $\hat{g}^A_\varepsilon$ it is easy to derive boundary conditions for Eq. (3.14). In a normal reservoir $\Delta = 0$ and $\hat{g}^A_\varepsilon = -\hat{\sigma}_z$. In a superconducting terminal having phase ϕ, $\Delta = |\Delta_S| e^{i\phi}$ and the Green function satisfies $\hat{g}^A_\varepsilon = \hat{\sigma}_x \sin\phi + \hat{\sigma}_y \cos\phi$.

It is also possible to simplify Eq. (3.12) for the distribution functions considerably: In the case of a negligible supercurrent $I_S = \int j_\varepsilon d\varepsilon$ the equations for the two distribution functions decouple, reducing f_L to its equilibrium value $f_L = \tanh(\varepsilon/2T)$ and leaving us with a single equation for f_T which can be cast into the form of a diffusion equation:[17]

$$\boldsymbol{\nabla}(D(\varepsilon, \mathbf{r})\boldsymbol{\nabla} f_T(\varepsilon, \mathbf{r})) - \gamma(\varepsilon, \mathbf{r}) f_T(\varepsilon, \mathbf{r}) = 0, \tag{3.17}$$

where the first term describes diffusion of quasiparticles with an effective diffusion coefficient

$$D(\varepsilon, \mathbf{r}) = \frac{\mathscr{D}}{4}\mathrm{Tr}\{\hat{1} - \hat{\sigma}_z \hat{g}^R_\varepsilon \hat{\sigma}_z \hat{g}^A_\varepsilon\},$$

$$= \frac{\mathscr{D}}{8}\mathrm{Tr}\{(\hat{g}^A_\varepsilon + \hat{g}^{A\dagger}_{-\varepsilon})^2\}, \tag{3.18}$$

that is modified by the penetrating superconductivity. Here we have used the identity $\hat{g}^R_\varepsilon = -\hat{\sigma}_z \hat{g}^A_{-\varepsilon}\hat{\sigma}_z$, which relates the advanced and retarded Green functions. The second term describes absorption of quasiparticles in the superconducting condensate with a coefficient $\gamma = i/2\,\mathrm{Tr}\{(\hat{g}^R_\varepsilon + \hat{g}^A_\varepsilon)\hat{\Delta}\}$. In the absence of external fields γ is proportional to the local value of the pair potential, since in that case we can always choose Δ to be real, and we obtain

$$\gamma(\mathbf{r}, \varepsilon) = -\frac{i}{2}\Delta(\mathbf{r})\mathrm{Tr}\{i\hat{\sigma}_y(\hat{g}^A_{-\varepsilon} + \hat{g}^A_\varepsilon)\}. \tag{3.19}$$

The boundary conditions for Eq. (3.17) follow from expanding $\tanh[(\varepsilon + eV)/2T]$ to first order in V. This determines the boundary condition for f_T. In a normal reservoir that is biased at a (small) voltage V with respect to a superconducting lead, the distribution function is $f_T = (eV/2T)\cosh^{-2}(\varepsilon/2T)$.

In most theoretical approaches, see e.g., Refs. 3, 4, 10, and 27, electron-electron interactions in the normal metal are disregarded, leading to $\Delta, \gamma = 0$. However, as shown in Ref.

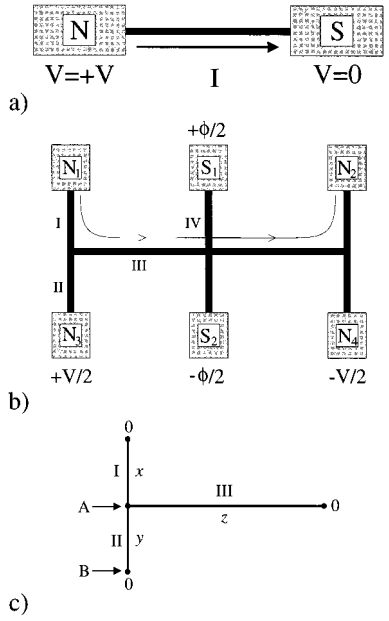

FIG. 2. (a) The simplest possible system, consisting of a diffusive normal metal wire of length L, that is connected on the left to a normal reservoir and to the right to a superconducting one. (b) An example of a more complicated structure. The branches I, II, and IV have length L', branch III has length L. For further details, see text. (c) The coordinates on the branches. The origins are indicated for each branch.

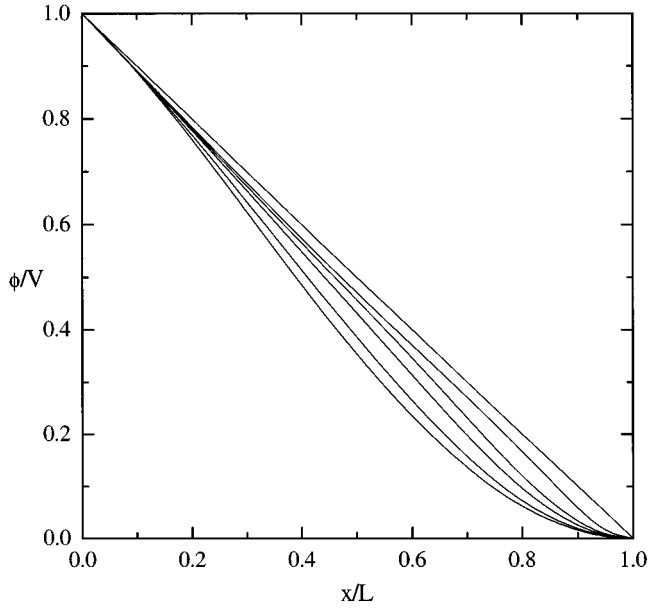

FIG. 3. Electrical potential distribution in the wire of Fig. 2(a) as a function of temperature. Going from bottom to top, the curves correspond to values of $L/\xi=0$, 1.0, 1.5, 2.0, 4.0, and ∞. The temperature is proportional to $(L/\xi)^2$.

17, including the effect of these interactions produces a change in the resistance. We thus need Eq. (3.13) for Δ, which after a straightforward calculation can be rewritten as

$$\Delta=\frac{\lambda}{8i}\int d\varepsilon\tanh\left(\frac{\varepsilon}{2T}\right)\mathrm{Tr}\{i\hat{\sigma}_y(\hat{g}^A_\varepsilon-\hat{g}^R_\varepsilon)\}. \qquad (3.20)$$

We now have all the necessary ingredients to calculate the various nonequilibrium transport properties of the system. The next section will be devoted to two of these properties, namely the electrostatic and chemical potential distributions.

IV. ELECTROSTATIC VERSUS CHEMICAL POTENTIAL

As a first example of the theory of Sec. III we calculate the electrostatic and the chemical potential in the 1D wire of Fig. 2(a). As was shown above, the former is determined by the distribution of electric charge in the wire. The latter determines the magnitude of the current that flows through the sample. The system consists of a diffusive normal metal wire of length L attached on the left to a normal metal reservoir and on the right to a superconducting terminal. The normal lead is biased at a small voltage V with respect to the superconductor. The normal reservoir is situated at $x=0$.

Using Eq. (3.11) for the Keldysh component and Eq. (3.15) for the Green function we obtain

$$\varphi(x)=\frac{1}{e}\int_0^\infty d\varepsilon f_T(x,\varepsilon)\cos(\theta(x,\varepsilon)). \qquad (4.1)$$

In Fig. 3 we have calculated the potential distribution in the normal metal for different values of L/ξ, i.e., for different temperatures.

In the limiting cases of low and high temperatures, the potential can be calculated analytically:

$$\varphi(x)=V\left(1-\frac{x}{L}\right)\cos\left(\frac{\pi x}{2L}\right), \quad T\to 0, \qquad (4.2a)$$

$$\varphi(x)=V\left(1-\frac{x}{L}\right), \quad \frac{\mathscr{D}}{L^2}\ll k_BT\ll\Delta_S. \qquad (4.2b)$$

Figure 3 shows that the potential distribution changes with temperature from a nontrivial one which is influenced strongly by the penetrating superconductivity to the expected linear dependence for high temperatures (but still $k_BT\ll\Delta_S$). This behavior is caused by the fact that the density of states vanishes in the vicinity of the superconductor. Hence, the charge distribution which causes the electrostatic potential also vanishes in this region. The most important consequence of the nonlinear voltage distribution across the sample is the fact that the resistance at a certain point is no longer local, but depends on the distribution of resistivity in the entire structure. This is a direct consequence of the coherent nature of Andreev reflection as was discussed above.

The chemical potential, which is simply proportional to the energy integrated distribution function, is much less sensitive to changes in temperature. The zero and high temperature distributions are the same and are given by

$$\mu_0(x)=V\left(1-\frac{x}{L}\right). \qquad (4.3)$$

In Fig. 4 we have plotted the deviation of the chemical potential from this zero temperature solution. First of all we note that the change is very small. The maximum change at first increases rapidly with increasing temperature. However, beyond a certain temperature, $L/\xi\approx 4$, the maximum starts

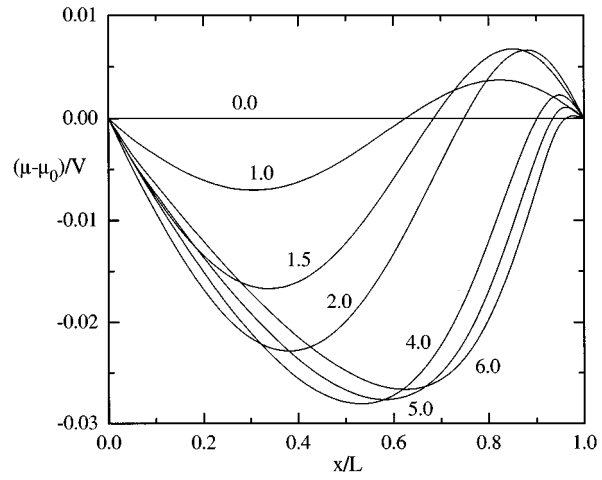

FIG. 4. Change in the chemical potential for the wire of Fig. 2(a) relative to the (linear) zero temperature distribution as a function of temperature. The labels near the curves indicate the value of L/ξ.

decreasing slowly. For high temperatures, the solution returns to the linear distribution. Thus we see that the electrostatic and chemical potential are only equal in the case of high temperatures, when both reduce to the trivial linear dependence that is also exhibited in the case of two normal terminals.

To indicate more clearly the difference between electrostatic and chemical potential, we have plotted the ratio of the two for different temperatures in Fig. 5. The electrostatic and chemical potential differ most at low temperatures and near the superconductor. However, in the vicinity of the normal reservoir they are almost equal and the extent into the wire at which they are equal increases at higher temperatures. In the high-temperature limit they both reduce to the same linear distribution, as was shown above.

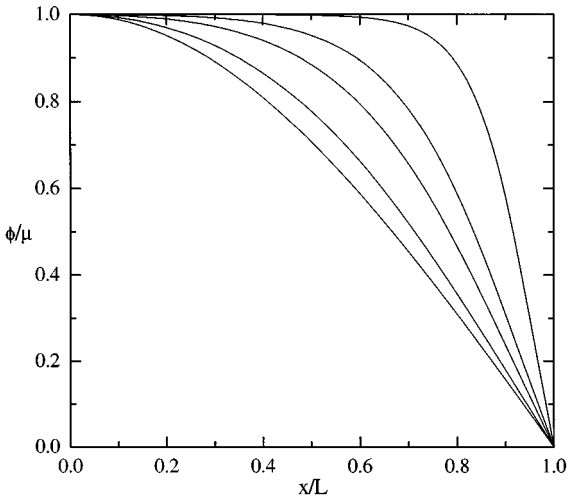

FIG. 5. The ratio of electrostatic and chemical potential as a function of temperature. Going from bottom to top, the curves correspond to values of $L/\xi=0$, 1.0, 1.5, 2.0, and 4.0.

V. THE INTERACTION EFFECT

A. The resistance of a 1D wire

In this section we calculate the resistance change at zero temperature due to the penetration of the pair potential into the normal metal region. We first consider the wire of Fig. 2(a) and then address more general geometries. In order to simplify the equations later on, the superconducting end of the wire is now located at $x=0$ and the normal end at $x=L$.

We first solve Eq. (3.14) for $\hat{g}^A$ numerically to zeroth order in Δ and φ:

$$\mathscr{D}\boldsymbol{\nabla}(\hat{g}^A_\varepsilon\boldsymbol{\nabla}\hat{g}^A_\varepsilon)-i\varepsilon[\hat{\sigma}_z,\hat{g}^A_\varepsilon]=0, \tag{5.1}$$

where $\varphi=0$ (zero voltage limit) and Δ has been disregarded since it is small in the normal metal region because of its proportionality to the interaction parameter λ. We then solve Eq. (3.17) to first order in γ. At zero temperature, $D(\varepsilon,x)=\mathscr{D}$, and we write $f_T=f_0+f_1$ with $f_1\ll f_0$. Then $f_0=c(\varepsilon)x/L$ and $f_1''=(\gamma/\mathscr{D})f_0$, with $c(\varepsilon)=(eV/4T)\cosh^{-2}(\varepsilon/2T)$. Using the fact that $\int_0^L f_1'(x')dx'=0$ $(f_1(0)=f_1(L)=0)$ we find

$$f_0'(L)=\frac{c(\varepsilon)}{L}, \tag{5.2a}$$

$$f_1'(L)=\frac{c(\varepsilon)}{\mathscr{D}L^2}\int_0^L x^2\gamma(x)dx. \tag{5.2b}$$

The current in a normal piece of metal is proportional to the local gradient of f. Since everywhere in the diffusive wire there is an induced pair potential it is not possible to calculate the current in this way somewhere in the middle of the wire. We must calculate it at the normal reservoir, where the pair potential is forced to vanish. The current flowing out of the normal reservoir (and hence the conductance G of the system) is therefore proportional to $f'(L)$. Noting that $\delta R/R=-\delta G/G$ we obtain for the relative resistance change:

$$\frac{\delta R}{R}=-\frac{f_1'(L)}{f_0'(L)}=-\frac{1}{\mathscr{D}L}\int_0^L dx x^2\gamma(x), \tag{5.3}$$

where γ is given by

$$\gamma(x)=2\Delta(x)\sin(\theta(\varepsilon=0,x)). \tag{5.4}$$

Thus the relative resistance change is proportional to the interaction parameter λ and its sign depends on the sign of λ. Here we use the convention that λ is positive for attractive effective interactions in the metal. Furthermore, the resistance change depends sensitively on the precise geometry of the structure, as will be shown in more detail in the next section. A measurement of this resistance change would allow one to directly measure λ. Calculating the relative resistance change for the wire of Fig. 2(a) gives

$$\frac{\delta R}{R}=-1.38\lambda, \tag{5.5}$$

independent of $\mathscr{D}$ and L. For silver, the estimated value of the interaction parameter is $\lambda=+0.04$ (Ref. 28), and there-

fore the resistance of a silver wire in contact with a superconductor is reduced by 5.5% with respect to its normal state value.

B. Generalization to arbitrary geometries

The results obtained above are readily generalized for arbitrary structures containing a number of normal reservoirs, two superconducting ones and a number of diffusive wires connecting them. To illustrate how the resistance change for such systems is calculated we consider the geometry shown in Fig. 2(b). This is a structure similar to the one we used recently[17] to model the experimental setup of Ref. 15. In the experiment a current was applied along the path indicated by the arrow going from normal lead N_1 to normal lead N_2. The voltage was measured between the opposite normal reservoirs N_3 and N_4. The superconductors have a phase difference ϕ. In principle Eqs. (3.14) and (3.17) should be solved in each branch of the structure and the solutions matched in every nodal point. However, it is possible to reduce this geometry to a one-dimensional one due to the symmetry of the geometry: The voltage and f_T distributions are antisymmetric with respect to the line S_1-S_2 in Fig. 2(b) whereas Δ and the Green function $\hat{g}_\varepsilon$ are symmetric. This allows us to consider only the three elementary branches I, III, and IV in the calculation of $\hat{g}_\varepsilon$.

For the calculation of the resistance change we need only consider the branches I and II, each having a length L', and III which has a length L. As depicted in Fig. 2(c) we use coordinates x, y, and z to denote the position on branch I, II, and III, respectively. with the origins as indicated. The zeroth-order solution of Eq. (3.17) is

$$f_0=\begin{cases} L+L'-x & \text{(I)},\\ L & \text{(II)},\\ z & \text{(III)}. \end{cases} \tag{5.6}$$

Integrating $f_1''=(\gamma/\mathscr{D})f_0$ in each branch gives

$$f_1'=\begin{cases} c_1+\displaystyle\int_0^x dx'(L+L'-x')\frac{\gamma(x')}{\mathscr{D}} & \text{(I)},\\ c_2+\displaystyle\int_0^y dy' L\frac{\gamma(y')}{\mathscr{D}} & \text{(II)},\\ c_3+\displaystyle\int_0^z dz' z'\frac{\gamma(z')}{\mathscr{D}} & \text{(III)}. \end{cases} \tag{5.7}$$

Here the integration constant $c_1=0$ because the current in point $x=0$ is fixed and $c_2=0$ because there is no current in branch II. Note that the situation here is different from the one in Sec. V A. There we calculated the change in current at fixed voltage whereas in this case we calculate the voltage change at fixed current. Consequently the resistance change is now given by $\delta R/R=\delta V/V=f_1(B)/f_0(B)$. In the nodal point A we have $f_1'(x=L')+f_1'(y=L')+f_1'(z=L)=0$ and this gives

$$c_3+\int_0^L dz\frac{z\gamma(z)}{\mathscr{D}}+\int_0^{L'} dy\frac{L\gamma(y)}{\mathscr{D}}+\int_0^{L'} dx\frac{(L+L'-x)\gamma(x)}{\mathscr{D}} =0. \tag{5.8}$$

The distribution function f_1 in point A is now given by

$$f_1(A)=c_3\int_0^L dz+\int_0^L dz\int_0^z dz'\frac{z'\gamma(z')}{\mathscr{D}} =c_3L+\int_0^L dz\frac{Lz-z^2}{\mathscr{D}}\gamma(z). \tag{5.9}$$

Analogously we find for $f_1(B)$:

$$f_1(B)=f_1(A)-\int_0^{L'} dy\int_0^y dy'\frac{Ly'\gamma(y')}{\mathscr{D}} =f_1(A)-\int_0^{L'} dy\frac{y^2-LL'}{\mathscr{D}}\gamma(y). \tag{5.10}$$

Using Eq. (5.8) to eliminate the first two terms in expression (5.9) for $f_1(A)$ we calculate the resistance change:

$$\frac{\delta R}{R}=\int_0^{L'} dy\left(\frac{y^2}{L}-L-L'\right)\frac{\gamma(y)}{\mathscr{D}}-\int_0^L dz\frac{z^2\gamma(z)}{\mathscr{D}L} -\int_0^{L'} dx\frac{(L+L'-x)\gamma(x)}{\mathscr{D}}. \tag{5.11}$$

The relative resistance change depends on the phase difference ϕ between the superconductors through γ, which in its turn depends on ϕ via the boundary conditions imposed on $\hat{g}_\varepsilon$. Note that although branch IV does not enter the calculation of the resistance change, its length does influence the Green function, hence γ, and thus also the resistance of the structure.

Before discussing the results of a calculation for an experimentally relevant geometry, it is instructive to look at the (slightly unrealistic) case of constant γ to investigate the qualitative behavior of the system. In this case the resistance change reduces to

$$\frac{\delta R}{R}=\frac{\gamma L^2}{\mathscr{D}}\left(\frac{1}{3}\alpha^3-\frac{3}{2}\alpha^2-2\alpha-\frac{1}{3}\right) \quad \text{with} \quad \alpha=\frac{L'}{L} \tag{5.12}$$

which shows that, since $\gamma\sim\lambda\mathscr{D}/L^2$, the relative resistance change is proportional to the interaction parameter and independent of the absolute values of L, L', and $\mathscr{D}$. Only the ratio of L and L' is important. In this simple case the largest effect would be obtained for $\alpha=3.56$. We can get an idea how sensitive the resistance change is to the details of the geometry by comparing the cross structure ($L'=0$) with the structure in which $L'=L$. It is easily calculated that the resistance change is higher in the latter case by a factor of 10.5, showing that a relatively small change in geometry causes a major modification of the resistance change. In a realistic computation the modification due to these side branches is not so dramatic, but is still about a factor 3.

The result of such a realistic calculation is depicted in Fig. 6 where the scaled resistance change has been plotted for the Andreev interferometer of Fig. 2(b) with $L_I=L_{II}=L_{III}=L_{IV}=L$. This layout is similar to the one we used in Ref. 17 to model the experimental setup of Petrashov *et al.*[15]

There are two main differences with the previous results for the one-dimensional wire. The first is the dependence of

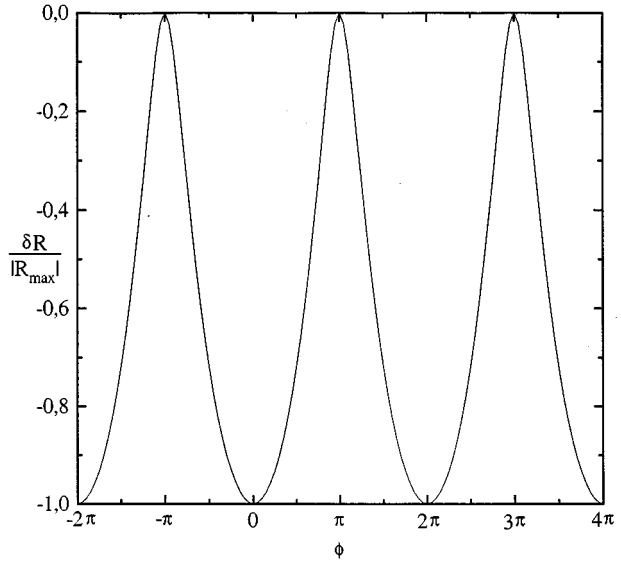

FIG. 6. The scaled resistance change due to the interaction effect of the structure shown in Fig. 2(b) with $L_I=L_{II}=L_{III}=L_{IV}=L$. The magnitude of the effect is 0.9%.

the resistance change on the phase difference ϕ between the superconductors with oscillation period 2π. The effect has its largest (negative) value for zero phase difference and vanishes for a phase difference of π, when superconductivity in the current branch (branches I, II, and their mirror images) is completely suppressed. The second difference is the magnitude of the effect. In the one-dimensional case this was 5.5%. Here it is 0.9% (for silver). Although this value is proportional to the interaction parameter and strongly depends on the length of the branches I and II, as was established above, a more important reason in this case is that the superconductors are not in the current path. As a consequence, the pair potential in branches I and II is smaller than in the one-dimensional case, leading to a weaker effect. In general, the magnitude of the interaction effect is smaller than the influence of a finite temperature on the resistance. This latter phenomenon is the subject of the next section.

VI. THE THERMAL EFFECT

A. The temperature-dependent resistance of a 1D wire

As was shown recently by the authors,[17] the experimental results of Ref. 15 could be explained by the temperature-dependent proximity effect. In this case no pair potential is induced in the normal metal region by the electron-electron interaction but coherence occurs as a result of the finite extent $\xi=\sqrt{\mathscr{D}/T}$ at which the superconductivity penetrates into the normal metal. Although the implications of this effect for complex structures are not always immediately apparent, the mechanism itself is not new. It was already studied in the middle seventies[16] and is in fact the phenomenon of Andreev reflection in diffusive metals. In spite of the fact that the effect has been known for a long time, a clear physical picture is still lacking.

To describe this effect we disregard the second term in Eq. (3.17) but we now take into account the fact that at finite temperatures the effective diffusion coefficient is no longer constant but depends on energy and position: $D(\varepsilon,x)=(\mathscr{D}/8)\mathrm{Tr}\{[\hat{g}^{\mathrm{A}}_{\varepsilon}(x)+\hat{g}^{A\dagger}_{-\varepsilon}(x)]^2\}$. The diffusion coefficient reduces to $\mathscr{D}$ for low and high energies. For energies $\varepsilon\approx\mathscr{D}/L^2$ it exhibits a maximum which is about twice as large as the zero energy value. The temperature enters the boundary conditions for Eq. (3.17), but more importantly it determines the energy window in which the quasiparticles experience the energy dependence of the diffusion coefficient. Therefore the resistance change should vanish at both low and high temperatures and have a minimum for quasiparticle energies $\varepsilon\approx\mathscr{D}/L^2$.

As in the previous section, we will first calculate this effect for the one-dimensional structure of Fig. 2(a) and then extend the treatment to more general structures, using the geometry of Fig. 2(b) as an example. The normal lead is now situated at $x=0$ and the superconducting one at $x=L$. The procedure is as follows. We first integrate the diffusion equation for f_T twice, which gives $f_T(x,\varepsilon)=a(\varepsilon)\int_0^x D^{-1}(x',\varepsilon)dx'+b(\varepsilon)$. The integration constants may still depend on ε and are determined by the boundary conditions $f_T(0,\varepsilon)=(eV/2T)\cosh^{-2}(\varepsilon/2T)$ and $f_T(L,\varepsilon)=0$. This gives

$$f_T(x,\varepsilon)=\frac{eV}{2T}\cosh^{-2}\left(\frac{\varepsilon}{2T}\right)\left(1-\frac{m(x,\varepsilon)}{m(L,\varepsilon)}\right) \tag{6.1}$$

with

$$m(x,\varepsilon)=\frac{1}{L}\int_0^x D^{-1}(x',\varepsilon)dx'. \tag{6.2}$$

As before, the current flowing out of the normal contact is proportional to $f_T'(0,\varepsilon)$ and hence we obtain for the normalized conductance G/G_N:

$$\frac{G}{G_N}=\frac{1}{2\mathscr{D}T}\int_0^\infty d\varepsilon m^{-1}(L,\varepsilon)\cosh^{-2}\left(\frac{\varepsilon}{2T}\right)$$
$$=\frac{\xi^2}{2L^2\mathscr{D}}\int_0^\infty d\tilde{\varepsilon}m^{-1}(L,\varepsilon)\cosh^{-2}\left(\frac{\tilde{\varepsilon}\xi^2}{2L^2}\right), \tag{6.3}$$

where we have used $T=\mathscr{D}/\xi^2$ and scaled the energy with the Thouless energy $\tilde{\varepsilon}=\varepsilon L^2/\mathscr{D}$. Note that the $\cosh^{-2}(\varepsilon/2T)$ part of the integrand defines the energy interval in which the quasiparticles feel the energy dependence of $m^{-1}(L,\varepsilon)$, as mentioned above. Equation (6.3) shows that the normalized conductance depends on the ratio $L/\xi\sim\sqrt{T}$ only (the factor $[\mathscr{D}m(L,\varepsilon)]^{-1}$ is dimensionless and does not depend on temperature). In Fig. 7 the temperature dependence of the normalized resistance, $R/R_N=G_N/G$, is plotted. As expected, the effect vanishes at $T=0$ and for $T\to\infty$. The maximum magnitude of the temperature effect is material independent and in general larger than that of the interaction effect; 10% vs 5.5% for the particular case of a silver wire. Although the high temperature tail such as the one of Fig. 7 was already observed in Ref. 15, the low-temperature reentrant behavior of the resistance had, until recently,[30] not yet been measured.

B. Temperature effect in Andreev interferometers

A generalization of this theory to more complicated structures should take into account how a resistance measurement

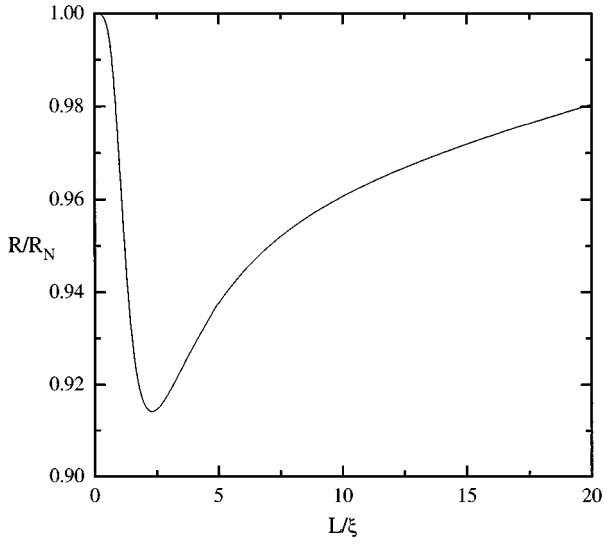

FIG. 7. Temperature dependence of the normalized resistance of the structure shown in Fig. 2(a). The temperature is proportional to $(L/\xi)^2$.

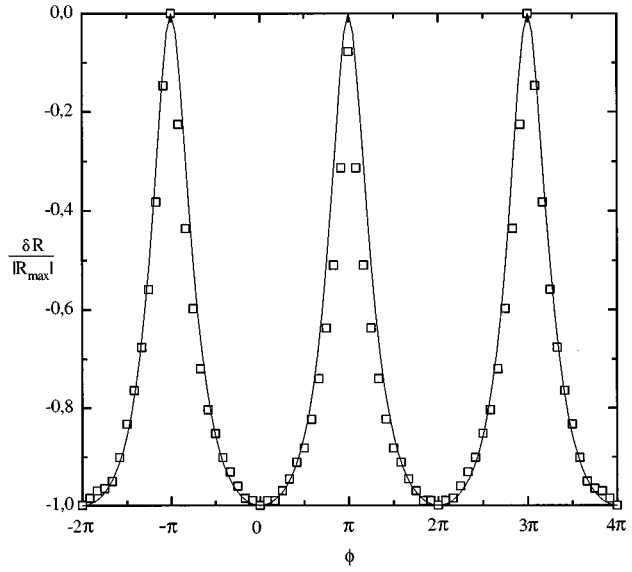

FIG. 8. Scaled resistance change due to the thermal effect of the structure shown in Fig. 2(b) with $L_I=L_{II}=L_{IV}=L$ and $L_{III}=2L$ for $L/\xi=3$. The magnitude of the effect is 9.7%. The squares are the experimental data of Ref. 15.

is actually done. In the case of the experiment of Ref. 15 a current was applied between N_1 and N_2 whereupon the voltage between N_3 and N_4 was measured (see Fig. 2). As a consequence, there is no current in branch II nor in its mirror image attached to reservoir N_4. To calculate the resistance of this complex structure we proceed as follows. We start by noting that the current is conserved for each quasiparticle energy ε. This implies that $\mathscr{T}_I(\varepsilon)+\mathscr{T}_{II}(\varepsilon)=\mathscr{T}_{III}(\varepsilon)$. We now apply standard circuit theory for every quasiparticle energy (we use the fact that due to the antisymmetry of the voltage distribution the voltage is zero in the middle of the structure):

$$\mathscr{V}_1(\varepsilon)=\mathscr{T}_I(\varepsilon).\mathscr{R}_I(\varepsilon)+\mathscr{T}_{III}(\varepsilon).\mathscr{R}_{III}(\varepsilon), \qquad (6.4a)$$

$$\mathscr{V}_3(\varepsilon)=\mathscr{T}_{II}(\varepsilon).\mathscr{R}_{II}(\varepsilon)+\mathscr{T}_{III}(\varepsilon).\mathscr{R}_{III}(\varepsilon), \qquad (6.4b)$$

where $\mathscr{V}_i(\varepsilon)=(V_i/2T)\cosh^{-2}(\varepsilon/2T)$ and the indices on $\mathscr{V}$ refer to the respective reservoirs and the indices on $\mathscr{T}$ and $\mathscr{R}$ refer to the appropriate branches. The proportionality constants $\mathscr{R}_{I,II,III}(\varepsilon)$ in the different branches can be deduced from the resistance of the branches connecting two reservoirs:

$$\mathscr{R}_{ij}(\varepsilon)=\frac{f_i(\varepsilon)-f_j(\varepsilon)}{f_i'(\varepsilon)-f_j'(\varepsilon)}, \qquad (6.5)$$

where i and j label the reservoirs at which the distribution functions are evaluated.

Using the current conservation condition, Eq. (6.4) can be cast into the form of a matrix equation $\vec{\mathscr{V}}(\varepsilon)=\mathscr{R}(\varepsilon).\vec{\mathscr{T}}(\varepsilon)$, where $\mathscr{R}(\varepsilon)$ is a (2×2) matrix relating the voltage and current vectors $\vec{\mathscr{V}}(\varepsilon)=(\mathscr{V}_1(\varepsilon),\mathscr{V}_3(\varepsilon))^{\mathrm{T}}$ and $\vec{\mathscr{T}}(\varepsilon)=(\mathscr{T}_I(\varepsilon),\mathscr{T}_{II}(\varepsilon))^{\mathrm{T}}$. Inverting the matrix equation and integrating over all energies gives $\vec{I}=G\vec{V}$, where $\vec{V}=(V_1,V_3)^{\mathrm{T}}$, $\vec{I}=(I_I,I_{II})^{\mathrm{T}}$, and the conductance matrix is given by $G=(1/2)T\int_0^\infty d\varepsilon.\mathscr{R}^{-1}(\varepsilon)\cosh^{-2}(\varepsilon/2T)$. We now impose the boundary condition mentioned above on the currents in branches I and II: $\vec{I}=(I,0)^T$. This gives a relation between V_1 and V_3 in terms of the matrix elements of G; $V_1=-(G_{22}/G_{21})V_3$, which in turn must be used to calculate the experimentally measured resistance of the structure: $R=2V_3/I=2[G_{12}-(G_{11}G_{22}/G_{21})]^{-1}$. The resistance depends again on the phase difference between the two superconducting reservoirs because of the boundary conditions imposed on the Green function.

In Fig. 8 we have plotted the results of this calculation for the previously used geometry of Fig. 2(b) with $L_I=L_{II}=L_{IV}=L$ and $L_{III}=2L$. This particular calculation was done for the value of $L/\xi=3$ which gave the largest effect. Also shown are the experimental results of Ref. 15.

Again we find 2π periodic oscillations such as in Fig. 6, but although the phase dependence looks similar there are some distinct differences. First of all the shape of the oscillations is different, especially near the minima, where the thermal effect produces less narrow peaks than the interaction effect. The amplitude of the thermal oscillations is material independent whereas that of Fig. 6 is proportional to the interaction parameter of the metal. Moreover, the maximal magnitude of the oscillations, 9.7% in this particular case, are in general much larger in the thermal effect, which makes observation of the previously discussed oscillations more difficult.

We obtain an excellent fit with the experimental data in Fig. 8, where the magnitude of the oscillations is about 11%. However, a decisive check on our theory would be provided by the observation of the temperature dependence of the resistance such as the one plotted in Fig. 7 for the system considered here. Indeed, unpublished data by the authors of Ref. 15 also show a remarkable agreement[29] with our calculations.[17] Moreover, very recently the observation of this reentrant behavior has been claimed by an independent experimental group.[30]

VII. SUMMARY

We have performed calculations of the distribution of the electrostatic and nonequilibrium chemical potential in a one-dimensional disordered superconducting hybrid wire. We showed that the two behave differently as a function of temperature and that they are in fact only equal in the high-temperature limit. We have proposed an experimental setup to measure these different potential distributions. We have also presented a computation for this wire using a recently developed[17] mechanism, that causes the resistance of a diffusive superconducting hybrid structure to change at zero temperature. The latter is in contrast with the well-known thermal mechanism of Andreev reflection in diffusive metals, where the resistance change vanishes for low temperatures. In addition to this result we have given a detailed account of the calculation performed in Ref. 17 for the experimental setup of Ref. 15. Since the relative resistance change due to the mechanism is proportional to the interaction parameter in the normal metal, observation of this effect would allow a direct measurement of this physical quantity. Furthermore, we have shown how to calculate the resistance of an arbitrary Andreev interferometer using finite-temperature proximity effect theory. Because the finite-temperature effect generally causes a much larger resistance change, this is the correct theory to describe an experiment such as the one performed in Ref. 15.

ACKNOWLEDGMENTS

The authors would like to thank Daniel Estève, Gerrit Bauer, Luuk Mur, Bart van Wees, Mark Visscher, and Henk Stoof for valuable discussions. This work is part of the research program of the ''Stichting voor Fundamenteel Onderzoek der Materie (FOM),'' which is financially supported by the ''Nederlandse Organisatie voor Wetenschappelijk Onderzoek (NWO).''

[1] A. F. Andreev, Sov. Phys. JETP **19**, 1228 (1964); **24**, 1019 (1967).
[2] G. E. Blonder, M. Tinkham, and T.M. Klapwijk, Phys. Rev. B **25**, 1415 (1982).
[3] C. J. Lambert, J. Phys. Condens. Matter, **3**, 6579 (1991).
[4] C. W. J. Beenakker, Phys. Rev. B **46**, 12 841 (1992).
[5] H. Nakano and H. Takayanagi, Solid State Commun. **80**, 997 (1991).
[6] F. W. J. Hekking and Yu. V. Nazarov, Phys. Rev. Lett. **71**, 1625 (1993).
[7] A. V. Zaitsev, Phys. Lett. A **194**, 315 (1994).
[8] A. Kadigrobov, A. Zagoskin, R. I. Shekhter, and M. Jonson, Phys. Rev. B **52**, 8662 (1995).
[9] N. K. Allsopp, J. Sanchez Canizares, R. Raimondi, and C. J. Lambert (unpublished).
[10] Yu. V. Nazarov, Phys. Rev. Lett. **73**, 1420 (1994).
[11] A. Volkov, N. Allsopp, and C. J. Lambert, J. Phys. Condens. Matter **8**, L45 (1996).
[12] P. G. N. de Vegvar, T. A. Fulton, W. H. Mallison, and R. E. Miller, Phys. Rev. Lett. **73**, 1416 (1994).
[13] H. Pothier, S. Guéron, D. Estève, and M. H. Devoret, Phys. Rev. Lett. **73**, 2488 (1994).
[14] A. Dimoulas, J. P. Heida, B. J. van Wees, T. M. Klapwijk, W. v.d. Graaf, and G. Borghs, Phys. Rev. Lett. **74**, 602 (1995).
[15] V. T. Petrashov, V. N. Antonov, P. Delsing, and T. Claeson, Phys. Rev. Lett. **74**, 5268 (1995).
[16] S. N. Artemenko, A. F. Volkov, and A. V. Zaitsev, Solid State Commun. **30**, 771 (1979).
[17] Yu. V. Nazarov and T. H. Stoof, Phys. Rev. Lett. **76**, 823 (1996).
[18] B. Z. Spivak and D. E. Khmelnitskii, JETP Lett. **35**, 412 (1982) [Pis'ma Zh. Éksp. Teor. Fiz. **35**, 334 (1982)].
[19] B. L. Altshuler, D. E. Khmelnitskii, and B. Z. Spivak, Solid State Commun. **48**, 841 (1983).
[20] F. Zhou, B. Spivak, and A. Zyuzin, Phys. Rev. B **52**, 4467 (1995).
[21] L. V. Keldysh, Sov. Phys. JETP **20**, 1018 (1964) [Zh. Éksp. Teor. Fiz. **47**, 1515 (1964)].
[22] A. I. Larkin and Yu. V. Ovchinnikov, Sov. Phys. JETP **41**, 960 (1975) [Zh. Éksp. Teor. Fiz. **68**, 1915 (1975)]; **46**, 155 (1977) [**73**, 299 (1977)].
[23] A. Schmid, *Nonequilibrium Superconductivity, Phonons and Kapitza Boundaries*, Proceedings of the NATO Advanced Study Institute, Acquafredda di Marathea, Italy, 1980 (Plenum, New York, 1981).
[24] J. Rammer and H. Smith, Rev. Mod. Phys. **58**, 323 (1986).
[25] A. A. Abrikosov, L. P. Gorkov, and I. E. Dzyaloshinski, *Methods of Quantum Field Theory in Statistical Physics* (Dover, New York, 1963).
[26] K. D. Usadel, Phys. Rev. Lett. **25**, 507 (1970).
[27] A. F. Volkov, A. V. Zaitsev, and T. M. Klapwijk, Physica C **210**, 21 (1993).
[28] A. C. Mota, P. Visani, and A. Pollini, J. Low Temp. Phys. **76**, 465 (1989).
[29] P. Delsing (unpublished).
[30] H. Courtois (unpublished).